Actin Dynamics, Regulated by RhoA-LIMK-Cofilin Signaling, Mediates Rod Photoreceptor Axonal Retraction After Retinal Injury

Weiwei Wang,* Eva Halasz, and Ellen Townes-Anderson

Department of Pharmacology, Physiology and Neuroscience, New Jersey Medical School, Graduate School of Biomedical Sciences, Rutgers Biomedical and Health Sciences, Rutgers, The State University of New Jersey, Newark, New Jersey, United States

Correspondence: Weiwei Wang, Grousbeck Gene Therapy Center, Schepens Eye Research Institute and Massachusetts Eye and Ear, Harvard Medical School, Boston, MA, USA; weiwei_wang@meei.harvard.edu.

Current affiliation: *Grousbeck Gene Therapy Center, Schepens Eye Research Institute and Massachusetts Eye and Ear, Harvard Medical School, Boston, Massachusetts, United States.

Submitted: October 27, 2018
Accepted: March 29, 2019

Citation: Wang W, Halasz E, Townes-Anderson E. Actin dynamics, regulated by RhoA-LIMK-cofilin signaling, mediates rod photoreceptor axonal retraction after retinal injury. *Invest Ophthalmol Vis Sci*. 2019;60:2274–2285. https://doi.org/10.1167/iovs.18-26077

Purpose. Retraction of the axon terminals of rod photoreceptors after retinal detachment breaks the first synapse in the visual pathway, resulting in visual impairment. Previous work showed that the mechanism of axonal retraction involves RhoA signaling and its downstream effector LIM Kinase (LIMK) activation. We examined the response of the downstream component cofilin, a direct binding protein of actin filaments, as well as the regulation by RhoA-LIMK-Cofilin signaling of actin assembly/disassembly, in the presynaptic ribbon terminal of injured rod cells.

Methods. Injury was produced by retinal detachment or rod cell isolation. Detached porcine retina was probed for levels and localization of phosphorylated cofilin with Western blots and confocal microscopy, whereas rod cell cultures of dissociated salamander retina were examined for filamentous actin assembly/disassembly with a barbed end assay and phalloidin staining.

Results. A detachment increased phosphorylation of cofilin in retinal explants; phosphorylation occurred in rod terminals in sections of detached retina. Isolation of rod cells resulted in axon retraction accompanied by an increase in actin barbed ends and a decrease in net filament labeling. All changes were significantly reduced by either Rho kinase (ROCK) or LIMK inhibition, using Y27632 or BMS-5, respectively. Cytochalasin D also reduced retraction and stabilized filaments in isolated rod cells.

Conclusions. These results indicate that actin depolymerization via activation of RhoA downstream kinases and cofilin contributes to axon retraction. Preventing depolymerization, in addition to actomyosin contraction, may stabilize ribbon synapses after trauma.

Keywords: rod photoreceptor, retinal injury, actin dynamics, RhoA signaling, LIMK

The cytoskeleton is key to nerve cell structure, most notably the axonal and dendritic extensions where synaptic connections are made. Therefore, its control contributes to development, maintenance, plasticity, and loss of synaptic connectivity.

In response to the injury of retinal detachment, rod photoreceptors retract their axonal fibers and synaptic terminals back into the outer nuclear layer (ONL), where their cell somata reside. Retraction of the terminal causes synaptic disjunction (as demonstrated with serial electron microscopic examination in detached cat retina[1]) and occurs as soon as 2 hours after detachment in detached pig retina.[2] This retraction has been observed in human patients as well as in animal studies.[3–7] In spite of a 90%-plus success rate in reattachment surgery, which fosters regrowth of photoreceptor outer segments,[8] visual acuity of 20/50 or better is obtained in only 20% to 40% of surgical patients.[9,10] It has been suggested that poor visual outcomes are likely due to disruption in retinal circuitry, such as the axon retraction by rod photoreceptors.[7,11] In addition to breaking the first synapse in the visual pathway, photoreceptor axonal retraction may be an initial step toward more complex remodeling by retinal cells through cell migration, rewiring of neuronal circuitry, and neuronal death in retinal disease.[12]

Our previous studies had shown that RhoA signaling increases after retinal detachment both in vitro and in vivo.[2,6] Moreover, inhibition of Rho kinase (ROCK) or its downstream effector LIM kinase (LIMK) reduced rod cell axonal retraction.[6,13] The RhoA-ROCK-LIMK pathway is well known for regulating the actin cytoskeleton.[14] Although many groups have studied actin dynamics in conventional synapses during synaptic plasticity and degenerative diseases, an examination has not been done of actin filament turnover in photoreceptor ribbon synapses. Unlike typical projection neurons, photoreceptors have structurally and physiologically distinct features, such as:

- Vesicle release is regulated by graded membrane potential changes, instead of action potentials,
- Vesicles are linked to ribbons through filaments that are not recognized by anti-actin antibodies,
- Type I and II synapsins, a protein family that connects vesicles with actin filaments in conventional synapses, cannot be detected in photoreceptors,
- The typical axonal microtubule binding protein, tau, is reported to be absent,

- Instead of N-type calcium channels, photoreceptor presynaptic terminals have L-type calcium channels,[15–17]
- Although axon terminals of photoreceptors contain the usual actin cytoskeleton, myosin V, in addition to myosin II isoforms are present in the presynaptic terminal.[11,15,18]

Thus, a specific study of photoreceptors is necessary to understand the role of actin filament assembly/disassembly and related signaling pathways in synaptic disjunction during the retinal injury response.

We have examined the phosphorylation of cofilin, a substrate of LIMK, and actin filament dynamics in detached retina and isolated rod cells. Additionally, we tested the effects of ROCK and LIMK inhibition and cytochalasin D on axon retraction. Our results confirm that actin depolymerization is a component of the machinery that regulates injury-induced axon retraction by rod cells and suggest that preservation of the cytoskeleton would prevent disruption of the connectivity between photoreceptors and secondary neurons.

Methods

Animals

Eyes from Yorkshire pigs (6 months old, weighing 65 to 80 kg) were obtained from a local slaughterhouse (Green Village Packing Co., Green Village, NJ, USA) and placed on ice during transport to the lab. Retinal explants were obtained immediately upon receipt, about 2 hours after slaughter. Adult, aquatic-phase tiger salamanders (*Ambystoma tigrinum*, 18–23 cm in length) were used to obtain retinal cells. Salamanders were maintained at 5°C on a 12-hour light/12-hour dark cycle for 1 week before use. All protocols were approved by the Institutional Animal Care and Use Committee (IACUC) at Rutgers, the State University of New Jersey, New Jersey Medical School and were in strict compliance with the ARVO Statement for the Use of Animals in Ophthalmic and Vision Research.

Pharmacologic Reagents and Antibodies

BMS-5 (Bristol-Myers Squibb, New York, NY, USA), SYN-1024 (Synkinase, San Diego, CA, USA), Y27632 (C3912; Sigma, St. Louis, MO, USA), and Cytochalasin-D (C8273; Sigma) were dissolved in dimethyl sulfoxide (DMSO) before adding to culture medium. For cells and retinal explants, the final DMSO concentration was 0.5%.

The primary antibodies used were the following:

- Rabbit monoclonal phospho-cofilin antibody (3313; Cell Signaling Technology, Danvers, MA, USA; 1:100 dilution for immunohistochemistry and 1:1000 for Western blots),
- Rabbit monoclonal cofilin antibody (5175; Cell Signaling; 1:200 dilution for immunohistochemistry and 1:1000 for Western blots),
- Mouse monoclonal GAPDH (1D4) antibody (sc-59540; Santa Cruz Biotechnology, Dallas, TX, USA; 1:1000),
- Mouse monoclonal SV2 antibody (Developmental Studies Hybridoma Bank, Iowa City, IA, USA; 1:100),
- Mouse monoclonal rhodopsin (4D2) antibody (MABN15; Millipore, Billerica, MA, USA; 1:200),
- Alexa Fluor 488-conjugated mouse monoclonal anti-biotin IgG (200-542-211; Jackson ImmunoResearch, West Grove, PA, USA; 1:200).

The secondary antibodies used were:

- Peroxidase-conjugated goat anti-rabbit IgG (111-035-045; Jackson ImmunoResearch; 1:5000),
- Peroxidase-conjugated goat anti-mouse IgG + IgM (115-035-068; Jackson ImmunoResearch; 1:5000),
- Alexa Fluor 488 donkey anti-rabbit IgG (A21206; Life Technologies, Carlsbad, CA, USA; 1:1000),
- Alexa Fluor 647 goat anti-mouse IgG (A21236; Life Technologies; 1:1000).

Tissue and Cell Cultures

Porcine retinal explants were obtained as previously described.[19] The anterior segment and vitreous body of porcine eyes were removed, and retinal explants were produced with a 7-mm diameter trephine. To detach the retinas, the inner limiting membrane of the retina was overlaid with filter paper, and the neural retina was gently teased away from the underlying retinal pigment epithelium (RPE), choroid, and sclera, leaving the photoreceptor layer exposed. Because previous studies demonstrated quantitatively similar amounts of rod cell axonal retraction 24 hours after retinal detachment regardless of retinal region,[19] both the superior and inferior retinas were used. Specimens were incubated in 12-well dishes in Neurobasal Medium (21103-049; Life Technologies) supplemented with B-27 (17504-044; Life Technologies), and 1.37 mM glutamine at 37°C. Medium was aerated with a humidified mixture of 5% CO_2/95% O_2.

Rod photoreceptors were obtained from salamander retinal dissociation, as previously described.[17,20,21] Salamanders were decapitated, pithed, and enucleated. Retinas were digested in Ringer's solution containing 14 U/ml papain with agitation for 45 minutes (10108014001; Roche Life Science, Indianapolis, IN, USA). After rinsing and trituration, the cell suspension was plated onto glass coverslips coated with Sal-1 antibody (provided by Peter MacLeish, Morehouse School of Medicine, Atlanta, GA, USA) in 35-mm culture dishes as described.[22] Cultures were maintained in a dark, humidified incubator at 10°C in serum-free medium containing 108 mM NaCl, 2.5 mM KCl, 2 mM HEPES, 1 mM $NaHCO_3$, 1.8 mM $CaCl_2$, 0.5 mM NaH_2PO_4, 1 mM $NaHCO_3$, 24 mM glucose, 0.5 mM $MgCl_2$, 1 mM Na pyruvate, 7% medium199, 1× minimum essential (MEM) vitamin mix, 0.1× MEM essential amino acids, 0.1× MEM nonessential amino acids, 2 mM glutamine, 2 μg/mL bovine insulin, 1 μg/mL transferrin, 5 mM taurine, 0.8 μg/mL thyroxin, 10 μg/mL gentamicin, and 1 mg/mL bovine albumin (pH 7.7).

Western Blots

After different periods of incubation, the detached porcine retinal explants were homogenized and lysed in ice-cold RIPA buffer supplemented with Complete Protease Inhibitor cocktail (04693116001; Roche), 1 mM Na_3VO_4 and 10 mM NaF. The lysates were clarified with centrifugation, 14,000 rpm for 10 minutes at 4°C. Protein concentrations were determined with the Bradford protein assay. Total lysate was boiled for 5 minutes in 2× Laemmli sample buffer and loaded onto a 12% Mini-Protean TGX SDS-PAGE Gel (456-1041; Bio-Rad, Hercules, CA, USA). Equal amounts of lysate were loaded into each lane of the same gel; depending on the gel, the loaded lysate ranged from 6 to15 μg protein. Blots were probed with appropriate primary and peroxidase-conjugated secondary antibodies. SuperSignal West Femto Substrate (34094; Thermo Scientific, Somerset, NJ, USA) or SuperSignal West Dura Substrate (34077; Thermo Scientific) was used for detection. GAPDH was used as a loading control. Blots were scanned with FluorChem (8800; Alpha Innotech Corporation, San Leandro, CA, USA) and analyzed with ImageJ (version 1.46r; National Institutes of Health, Bethesda, MD, USA).

Investigative Ophthalmology & Visual Science

Immunohistochemistry and Actin Staining

Porcine retinal explants and salamander retinal cell cultures were fixed with 4% paraformaldehyde in 0.1M sodium phosphate buffer (PBS, pH 7.4) overnight at 4°C.

Retinal explants were embedded in 30% sucrose overnight at 4°C, frozen in Optimal Cutting Temperature Compound (#4583; Sakura, Torrance, CA, USA) and sectioned at 30 µm. Sections were blocked with blocking buffer (10% donkey serum in PBS), immunolabeled with appropriate primary antibodies overnight at 4°C, rinsed with PBS and incubated with fluorescent secondary antibodies at room temperature for 1 hour. All specimens of a single experiment were processed together. Control sections were processed simultaneously without primary antibodies. Specimens were mounted with ProLong Gold Antifade Mountant (P36930; Life Technologies) and sealed for further examination. One-micron optical sections were obtained with a laser scanning confocal microscope (LSM510; Carl Zeiss, Oberkochen, Germany), equipped with argon and helium/neon lasers, a 40x, 1.2 N.A. water immersion objective and a 63x, 1.4 N.A. oil immersion objective. Laser power, scan rate, objective, aperture and exposure time were unchanged throughout each experiment for all specimens. Enhancements in brightness and contrast were performed with ImageJ (version1.46r; National Institutes of Health) only for presentation purposes.

For double labeling of p-cofilin with either SV2 or rhodopsin antibodies, detached retina from a live pig was used. Detachments were made by subretinal injection of BSS following procedures previously described.[2] Tissue was fixed after 2 hours and sectioned as above. Primary antibodies were applied simultaneously, followed by appropriate secondary antibodies. Nuclei were stained with TO-PRO-3 Iodide (T3605; Thermo Scientific). Optical sections (0.5 micron) were obtained with a Nikon A1R confocal microscope using a 63x, 1.4 N.A oil immersion lens.

To visualize actin filaments of rod photoreceptors, fixed cell cultures were incubated with 1% BSA, followed by incubation with Phalloidin-Alexa 488 (A12379; Life Technologies) diluted in 1% BSA at room temperature for 1 hour and then rinsed with PBS.

Barbed End Assay

After retinal dissociation, rod photoreceptors were cultured at different periods of time, as described in results, followed by incubation for 3 minutes at 37°C with permeabilization buffer, which also contained biotin-labeled actin monomers. This step allows biotin-labeled actin monomers to be delivered into the cells and added to free barbed ends of actin filaments. The permeabilization buffer contained: 1× Fix Buffer (5 mM KCl, 137 mM NaCl, 4 mM $NaHCO_3$, 0.4 mM KH_2PO_4, 1.1 mM Na_2HPO_4, 2 mM $MgCl_2$, 5 mM PIPES (pH7.2), 2 mM EGTA, 5.5mM glucose), 0.05% saponin, and freshly prepared actin dilution buffer (0.4 µM biotin-actin (AB07; Cytoskeleton, Inc.), 0.2 mM HEPES (pH 7.5), 40 µM $MgCl_2$, 40 µM ATP). Cultures were flooded with 1× Fix Buffer to stop the nucleation of actin filaments at the barbed ends, followed by fixation with 3.7% paraformaldehyde in 1× Fix Buffer for 1 hour at room temperature, two rinses with 0.1 M glycine for 10 minutes, and three washes with 1% BSA in Tris-buffered saline (TBS) for 5 minutes each time. A blocking solution of 1%FBS/1%BSA/TBS containing 3 mM unlabeled phalloidin was applied for 1 hour, followed by incubation with fluorescent anti-biotin antibody to identify nucleation sites with biotin-labeled actin at the barbed ends of actin filaments. After washing 5× for 5 minutes with 1% BSA in TBS, cultures were mounted with ProLong Gold Antifade Mountant (P36930; Life Technologies) and sealed for further examination.

Image Analysis

One-micron optical sections were obtained of randomly chosen isolated rod cells using a 63×, 1.4 N.A. oil immersion objective. Laser power and scan rate were unchanged throughout a single experiment. Immunolabeling of barbed ends was analyzed with ImageJ by measuring the area of the fluorescent signal above a threshold that was determined by the background signals obtained with a negative control (anti-biotin omitted). The region of interest (ROI) is illustrated in the results and consists of the basal area of the cell. The ROI was the same for the analysis of phalloidin labeling, axon and basal cell soma. Background—that is, labeling without phalloidin—was determined for each experiment. Final results both for barbed ends label and phalloidin label were reported as the percentage of the area containing fluorescence above the threshold within the ROI of each rod cell. Results were normalized by setting the control group at 100%. Enhancements in brightness and contrast were performed only for presentation purposes.

Measurement of Axon Retraction in Isolated Cells

To examine axon retraction, a Zeiss inverted light microscope (Axiovert S100TV; Carl Zeiss), equipped with a motorized stage (Assy Stage 25; Cell Robotics, Inc., Albuquerque, NM, USA) and a 40×, 0.75 N.A. objective, was used to view retinal cultures. Rod photoreceptors were identified by morphology (cell shape and presence of an ellipsoid and axon terminal). Rod cells with axon terminals (20–23 per dish) were selected by brightfield microscopy within the first hour after cell plating by viewing the culture at an arbitrary location and then systematically scanning in rows. At 7 hours, the same cells were located again. Their images were captured with a charge-coupled device camera (XC 75CE; Sony, Japan).

Axon length was measured with ImageJ. Reduction in length, indicating retraction, was the difference between the axonal lengths at the 1st (L1) and 7th (L7) hour of the same cell. The percent decrease in length was calculated with the following formula: (L1-L7) ÷ L1 × 100%.

Statistics

Data were collected by an observer blind to the experimental conditions, analyzed with Student's *t*-test or 1-way analysis of variance with Tukey's post hoc test for all pair-wise multiple comparisons (GraphPad Prism5; GraphPad Software, La Jolla, CA, USA) and expressed as mean ± SEM. Significance was considered to be achieved at $P < 0.05$.

Results

Phosphorylation of Cofilin Increases After Retinal Detachment

In a previous study, we demonstrated that retraction of rod axonal fibers leads to separation of rod spherules from bipolar dendrites by 2 hours after detachment in pig retina.[2] We further showed that active LIMK, phosphorylated-LIMK, promotes axonal retraction by rod photoreceptor terminals after retinal detachment.[13] LIMK is an upstream regulator of cofilin that contributes to actin filament turnover. To understand the impact of retinal detachment on actin dynamics, we

first examined the phosphorylation of cofilin after the injury of retinal detachment.

We used porcine eyes to obtain detached retinal explants because of their large size, the availability of suitable antibodies against cofilin, and the fact that porcine retina is similar to human retina anatomically and physiologically.[2,23,24] Moreover, we have recently examined detached retina from the living pig[2,25] and can confirm that the explants have a morphological response very similar to the detached retina in vivo. As our previous studies have shown, porcine retinal explants demonstrate a significant number of retracted synaptic terminals after 24 hours of detachment.[6,13] Each animal was used to collect data from 0 to 24 hours after retinal detachment. One eye was used for samples 0, 1, 5, 10, 30, and 60 minutes after detachment, the other eye for data 0, 1, 3, 7, and 24 hours after detachment (Fig. 1A). The retinal samples at the 0-time point were considered to be the basal level of total (t-) and phosphorylated (p-) cofilin before injury and arbitrarily set at 1 for quantification (Fig. 1B). Western blots demonstrated that the relative amount of p-cofilin was very low at time 0. Immediately following retinal detachment, p-cofilin levels increased; the increase was significant 30 minutes after detachment and continued to increase over 24 hours. Total cofilin, in contrast, remained stable; there was no significant difference from 1 to 24 hours (Fig. 1).

The stable level of total protein indicates that the increased phosphorylation of cofilin can be attributed to the regulatory activity of its upstream signaling pathways, such as increased activity of its kinase, LIMK, and/or reduced activity of its phosphatase, Slingshot Homolog (SSH).

ROCK-LIMK Inhibition Reduces Cofilin Phosphorylation

To confirm the role of LIMK in cofilin phosphorylation after retinal detachment, we examined the effect of ROCK or LIMK inhibition. Y27632, a selective inhibitor of both ROCK1 and ROCK2, causes an induced-fit conformational change of ROCK, allowing contact at its phosphate loop in the catalytic domain, thus competing with ATP to antagonize ROCK activity.[26,27] For LIMK inhibition, we used BMS-5, an inhibitor with high selectivity for both LIMK1 and LIMK2.[28] Although currently the specific mechanism by which BMS-5 inhibits LIMK activity is unknown, studies have shown that it can inhibit cofilin phosphorylation and reduce MDA-MB-231 cancer cell and mesenchymal glioblastoma multiforme (GBM) cell invasion,[29,30] presumably due to the role of LIMK-cofilin in regulating actin cytoskeleton rearrangement.

We examined porcine retinal explants at 1 and 24 hours after detachment to test both the acute and long-term effects of drug treatment. Samples for both time points, with or without treatment, were obtained from the same eye. Control groups were arbitrarily set at 100%. Y27632 (30 μM) significantly reduced phosphorylation of cofilin after retinal detachment: 1-hour treatment reduced p-cofilin to 49% of the untreated levels, while 24 hours of ROCK inhibition decreased p-cofilin to 78% (Fig. 2A, left panels). The less robust although still significant reduction of p-cofilin 24 hours after Y27632 treatment may be due to the relatively short half-life of Y27632 (about 60–90 minutes in blood).[31] A similar effect occurred in the BMS-5 (30 μM) treated group: p-cofilin decreased to 57% and 68% of untreated levels 1 and 24 hours after BMS-5 treatment respectively (Fig. 2B, left panels). Total cofilin protein levels were stable with either Y27632 or BMS-5 treatment (Figs. 2A, 2B, right panels).

Our results demonstrate that inhibition of either ROCK or LIMK reduced phosphorylation of cofilin after retinal detachment without altering cofilin expression. Further, results suggest that the correlation between the injury of retinal detachment and cofilin phosphorylation is mediated through the RhoA-ROCK-LIMK pathway.

Phosphorylation of Cofilin Occurs in the Rod Synaptic Terminal After Retinal Detachment

Because Western blots reveal changes of cofilin phosphorylation in all layers of retina, immunohistochemistry of retina was conducted to confirm that phosphorylated cofilin occurs in photoreceptor synaptic terminals after retinal detachment. Retinal explants, attached to RPE, were fixed immediately after dissection to provide a baseline for the immunocytochemistry. Retinal explants detached from the RPE were fixed after a 2- or 24-hour incubation. Previous studies had shown that RhoA-GTP, the active form of RhoA, increases immediately after injury and peaks at 2 hours in porcine retinal explants (Wang J, et al. *IOVS* 2013;54:ARVO E-Abstract 2845).[2] In addition, as previously stated, retraction of synaptic terminals by rod cells in detached porcine retinas is clearly present at 24 hours. We chose the 2-hour time point to examine cofilin localization at the peak of the RhoA response and compared it with the late injury response at 24 hours.

Cofilin was found in all layers of undetached retinal explants, with more intense labeling in the inner retina and plexiform layers (Fig. 3A, image 1). Labeling for p-cofilin changed over time (Figs. 3A, images 2 through 4). In undetached retina, the p-cofilin signal was very low, except in some cell somata located in the inner nuclear layer. There was no p-cofilin label in the OPL. Two hours after detachment, p-cofilin labeling showed an apparent increase, and the label was now present in the OPL where the photoreceptor synaptic terminals reside. Twenty-four hour detached retinal explants had more intense labeling of p-cofilin throughout the retina than 2-hour explants, and the signal was more obvious in the somata of photoreceptors. The increase of p-cofilin labeling throughout the retina, as well as in rod terminals over time, is consistent with the Western blot results above.

Sections of detached retina from a live pig were double immunolabeled for phosphorylated cofilin and either SV2 or rhodopsin. SV2 labeling marks the synaptic terminals of neurons in the outer and inner plexiform (synaptic) layers (OPL and IPL) of the retina, whereas rhodopsin identifies rod photoreceptors. After detachment, rhodopsin mislocalizes and is present along all membranes of the rod cells, marking not only the outer segment but the cell body and synaptic terminal as well.[19] Double labeling with anti-SV2 confirmed that p-cofilin resides in photoreceptor axon terminals of the OPL (Fig. 3B, images 1 through 3). Double labeling of rod opsin and p-cofilin identified that some of these axon terminals belong to rod photoreceptors (Fig. 3B, image 4 arrows). It is very likely that cone terminals contain p-cofilin as well: The p-cofilin/SV2 double labeling was found throughout the OPL layer where both cone and rod terminals locate.

Our results not only confirm the correlation between retinal detachment and increased cofilin phosphorylation but also demonstrate the presence of p-cofilin in rod photoreceptors, especially in their axon terminals, after detachment. As cofilin is well known for regulating actin dynamics, this led us to the next question: How do the actin filaments respond to the injury in the axon terminals of rod cells while retraction occurs?

Actin Filament Assembly/Disassembly at Axon Terminals of Rod Photoreceptors

To study actin dynamics in the axon terminal of rod photoreceptors after injury, cultures of adult, isolated salaman-

Investigative Ophthalmology & Visual Science

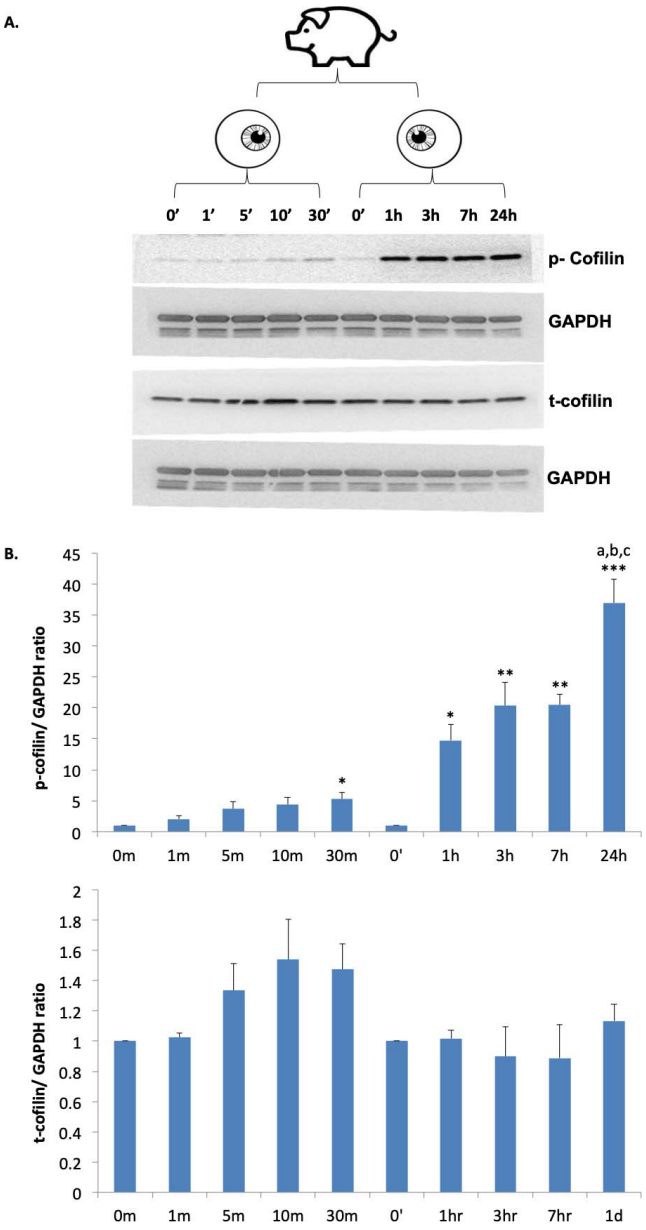

Figure 1. Phosphorylation of cofilin in porcine retinal explants increases after detachment over 24 hours while total cofilin remains stable. (**A**) Cofilin levels were examined within one animal: retinal explants incubated for 0, 1, 5 10, 30 minutes from one eye, 0, 1, 3, 7, 24 hours for the other eye. Antibodies against p-cofilin and t-cofilin labeled 19-kDa bands. GAPDH, from the same SDS-PAGE gel, served as an internal loading control. (**B**) Quantification of cofilin bands, normalized with GAPDH. $n = 3$ animals, 30 retinal explants; 1-way ANOVA compared within groups 0 to 30 minutes and 0 to 24 hours, $^{*}P < 0.05$, $^{**}P < 0.01$, $^{***}P < 0.001$; post hoc Tukey's test, a: 1 vs. 24 hours, <0.01, b: 3 vs. 24 hours, <0.05; b: 7 vs. 24 hours, <0.05.

der rod photoreceptors were used. Tiger salamander has been a reliable model for in vitro studies on photoreceptors.[20,22,32] Our previous work in utilizing salamander rod cells, demonstrated that the RhoA-ROCK/Pak-LIMK pathway regulates axonal and neuritic plasticity after injury.[5,33] In addition, retraction of the axon fiber by rod photoreceptors occurs over a 24-hour period in culture. Thus, porcine retinal explants and isolated salamander photoreceptors share similar timing and signaling components for axon retraction after injury.

We conducted a barbed end assay, which detects actin addition at the barbed ends of actin filaments and, by inference, the availability of barbed ends. Because cofilin severs actin filaments and generates barbed ends,[34] this experiment also provides information on cofilin activity. The procedure of detaching and dissociating retina before cell plating takes about 45 minutes. To allow for adequate attachment of cells to the culture substrate, the earliest time point we examined was 15 minutes after seeding. Thus, the earliest time that was examined was about 1 hour after the initial injury of retinal detachment.

Images of barbed end labeling in rod cells were obtained with confocal microscopy. Both rod cells with and without outer segments were present in the culture, as would occur in retinal detachment. Both types of rod cells showed retraction of the synaptic terminal and were used in analysis. The region of interest (ROI) for analysis included the axons and terminals, as well as the basal half of the cell soma into which the axons retract (Fig. 4A). The apical area of the cell soma was not included because the actin filaments there are enriched in calycal processes surrounding the inner segment (refer to Fig. 6A) and may be under a different regulatory mechanism. Calycal processes tend to form long filopodia after cells lose their outer segments in culture. In each experiment, the background signal due to nonspecific binding was determined by measuring the negative control group (no labeling of actin) and was used as the threshold for specific staining. We measured the area of the fluorescence signal above this threshold and reported its percentage of the area of the ROI for each cell.

The highest level of barbed end labeling occurred after 15 minutes of culture (Figs. 4B, 4C). Label at 15 minutes was arbitrarily set at 100%. After 2 hours in culture, the signal decreased to 65%, and after 4 hours was significantly decreased to 22% of the 15-minute label. Because the procedure of retinal dissociation itself introduces mechanical stress, an original baseline for rod cells without any injury could not be obtained. Nevertheless, our data reveal that the severing of actin filaments in the axon terminals was high in the 15-minute culture (approximately 1 hour after the initial injury), followed by a gradual decrease.

ROCK-LIMK Inhibition Reduces Actin Filament Disassembly After Injury

To understand the relationship of actin breakdown and ROCK-LIMK-cofilin activity after injury, we conducted barbed end assays with ROCK or LIMK inhibitors. As discussed, RhoA activation in porcine retinal explants is initiated immediately after retinal detachment even though peak activity occurs hours later (Wang J, et al. *IOVS* 2013;54:ARVO E-Abstract 2845).[2,6] During the procedure of dissecting salamander eyes and obtaining detached retinas, therefore, we assume that activated RhoA can lead to an immediate increase in ROCK activity and a subsequent increase in LIMK activity and p-cofilin. Thus, to examine the contribution of ROCK-LIMK activity at the inception of injury, we pretreated retina with kinase inhibitors before detaching the retinas.

Each experiment was conducted with one pair of salamander eyes: one eye pretreated with inhibitor, the other with a DMSO control. To deliver the treatment before detachment, two small cuts opposite each other were created at the edge of the cornea and the eyeballs incubated in Ringer's solution with inhibitor or DMSO for 20 minutes, followed by the standard retinal detachment and dissociation protocol. A barbed end assay was conducted 15 minutes after plating, consistent with the above experiments.

Investigative Ophthalmology & Visual Science

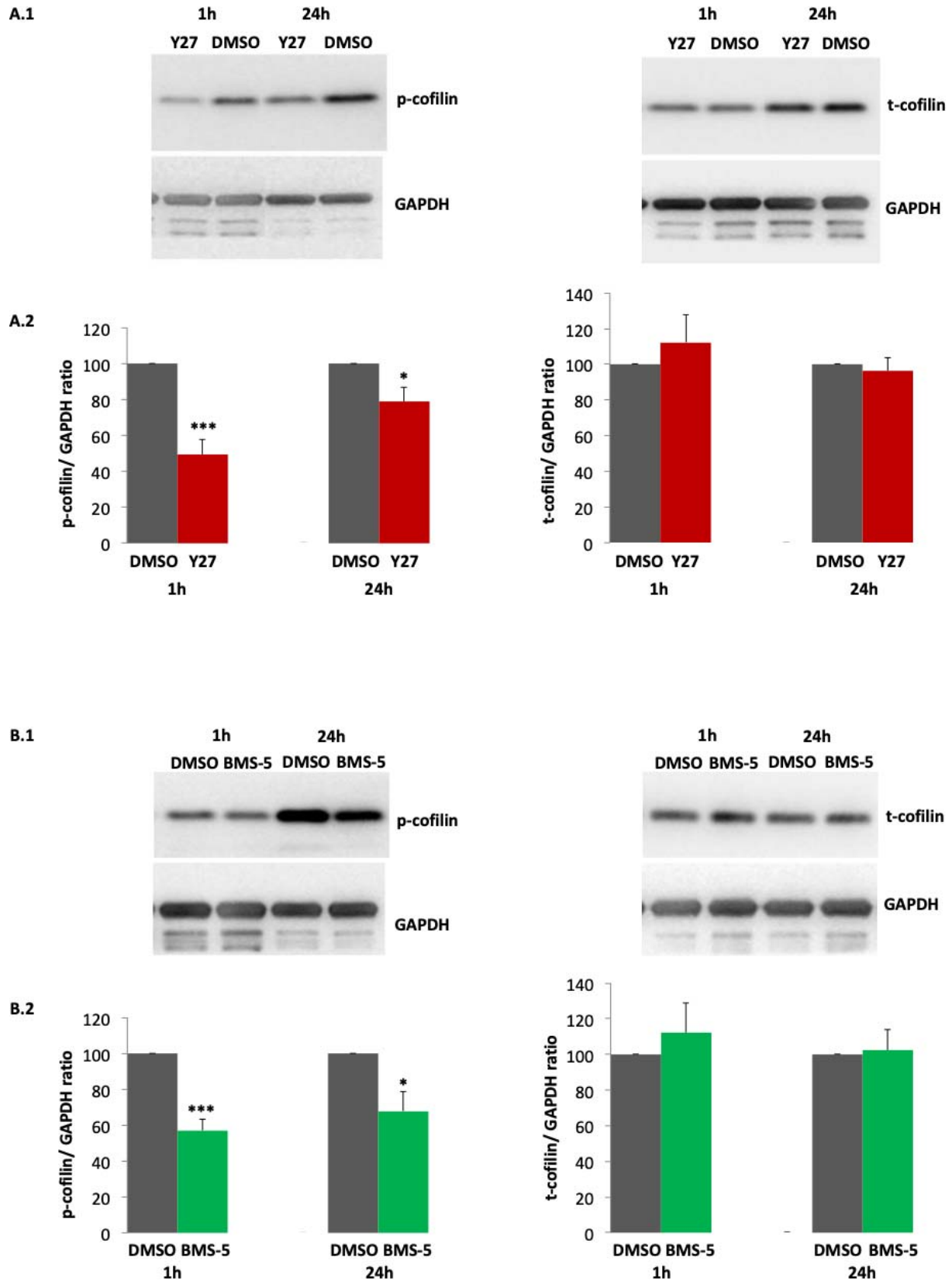

Figure 2. ROCK or LIMK inhibition, by 30 μM Y727632 (Y27) or 30 μM BMS-5 respectively, decreases phosphorylation of cofilin in porcine retinal explants 1 and 24 hours after detachment. Comparison between ROCK or LIMK inhibition and control was conducted with detached retinal explants from the same eyes. DMSO was the control condition (A.1, B.1). Antibodies against p-cofilin and t-cofilin labeled 19-kDa bands. GAPDH, from the same SDS-PAGE gel, served as an internal loading control. (A.2, B.2) Quantification of cofilin bands, normalized by GAPDH. Note, there was no change in t-cofilin with drug treatment. (**A**) $n = 4$ animals, 4 retinal explants per group; (**B**) $n = 4$ animals, 4 retinal explants per group; Student's *t*-test, $^{*}P < 0.05$, $^{***}P < 0.001$.

Investigative Ophthalmology & Visual Science

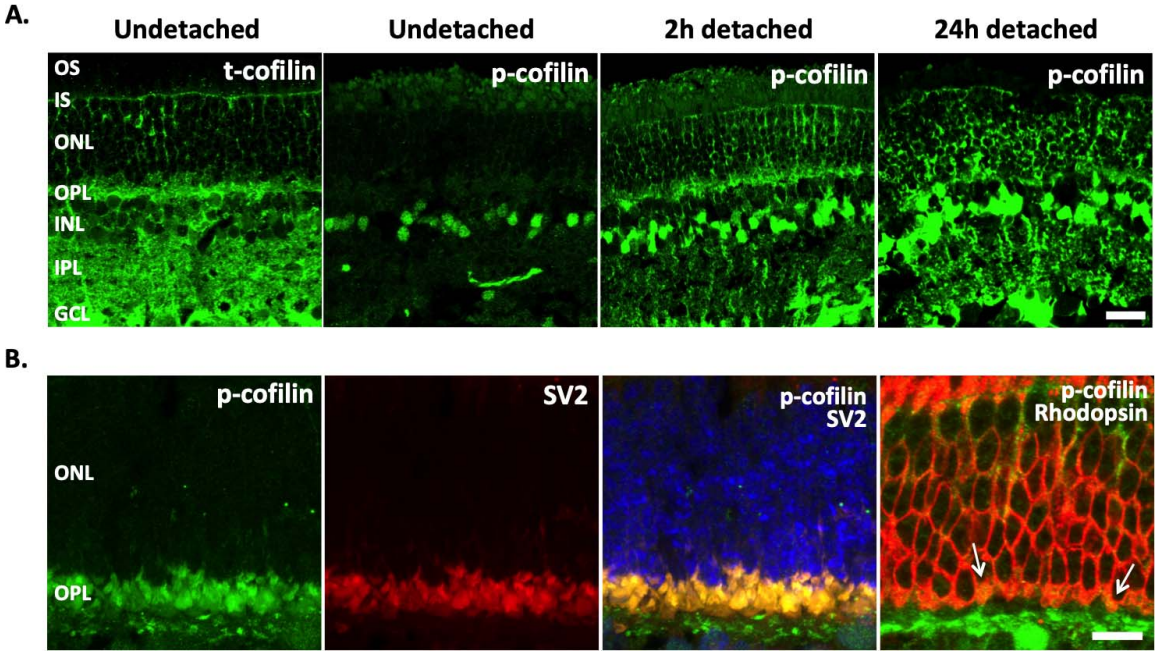

Figure 3. Distribution of total cofilin (t-cofilin) and phosphorylated (p-cofilin) in porcine retina examined with confocal microscopy. P-cofilin is detected in rod photoreceptor terminals after detachment. (**A**) Undetached, and 2 and 24 hours detached retinal explants. T-cofilin is present in all retinal layers. In normal, undetached retina, p-cofilin label was low throughout the retina except in some cells in the INL; after detachment, p-cofilin label increased throughout the retina. (**B**) Porcine retina from a live pig detached for 2 hours was labeled for p-cofilin (*green*), SV2 (*red*) or rod opsin (*red*), and nuclei (*blue*). SV2 colocalizes with p-cofilin in photoreceptor terminals, whereas opsin colocalizes with p-cofilin in the OPL; *arrows* highlight rod spherules in the outer synaptic layer. Opsin is present in the plasma membrane, p-cofilin is in the interior of the spherule. OS, outer segments; IS, inner segments; ONL, outer nuclear layer; OPL, outer plexiform layer; INL, inner nuclear layer; IPL, inner plexiform layer; GCL, ganglion cell layer. Optical sections, 1 μm in **A** and 0.5 μm in **B**. *Scale bars*: 20 μm (Fig. 3A), 10 μm (Fig. 3B).

Inhibition of ROCK or LIMK significantly reduced barbed end labeling in rod cells; there was an 87% reduction of barbed ends in the Y27632 (30 μM) treated group, while BMS-5 (10 μM) resulted in a 60% reduction compared to the control (Fig. 5). In each experiment, the DMSO group was arbitrarily set at 100%. These data indicate that the high level of barbed end labeling in the axon terminals of rod cells after injury was promoted (at least in part) through ROCK-LIMK activity. Since the Western blots and immunohistochemistry data above showed an increase of p-cofilin shortly after retinal detachment that is promoted by ROCK-LIMK activity, our results here are consistent with the well-recognized function of cofilin in severing actin filaments and producing barbed ends.[34–37]

Actin Filament Depolymerization During Axon Retraction

Although these results suggest a high level of actin filament turnover after injury, the overall structural change in the actin cytoskeleton remains to be investigated. Thus, we labeled actin filaments with Fluor 488 phalloidin, a specific stain for filamentous actin.

The same ROI was selected as above (Fig. 4A). The area of fluorescence signal (phalloidin labeling) in one-micron optical sections decreased in the terminal and adjacent cell soma; the 7-hour cultures had significantly less fluorescence than did cells in 2-hour cultures by 62.5% (Fig. 6). The time window of 2 to 7 hours in culture, or about 3 to 8 hours after retinal detachment, allowed us to examine actin cytoskeletal rearrangement during the most rapid phase of axonal retraction by cultured rod cells.[5] The decreased fluorescent signal suggested that actin filament depolymerization is occurring during axon retraction, although this does not rule out some level of polymerization. Inhibition of LIMK with BMS-5 (10 μM) prevented a decrease in phalloidin labeling (Fig. 6), indicating that depolymerization was under LIMK regulation.

Cytochalasin D Reduces Axon Retraction of Rod Photoreceptors After Injury

To further understand the relationship between axon retraction and actin depolymerization, we applied Cytochalasin D (Cyto D), a cell-permeable compound widely used for manipulating actin dynamics due to its ability to bind barbed ends of actin filaments with high affinity, as well as actin monomers with lower affinity.[38,39] This approach allowed us to directly disrupt actin depolymerization after injury, thus revealing the contribution of actin filament rearrangement to the synaptic structural plasticity of photoreceptors induced by injury.

We observed that Cyto D treatment increased the area of fluorescence signal for actin filaments (phalloidin labeling) in the terminals and adjacent cell somata during axon retraction, in contrast to the decrease of fluorescence signal in the untreated group.

As Figure 7A demonstrates, when fluorescence signal of the 2-hour untreated group is normalized to 100%, the 7-hour Cyto D group shows a significant 91.7% increase in the area with labeling. Because the fluorescence signal of phalloidin labeling is indicative of filamentous actin, this result suggests that Cyto D reduced actin depolymerization in photoreceptor axon terminals induced by injury. A significant effect of Cyto D on the preservation of axonal structure (Fig. 7B) was observed as well: In the Cyto D-treated group, the reduction of axon length over 7 hours after isolation was only 40% of the untreated group. Retraction had been reduced.

Investigative Ophthalmology & Visual Science

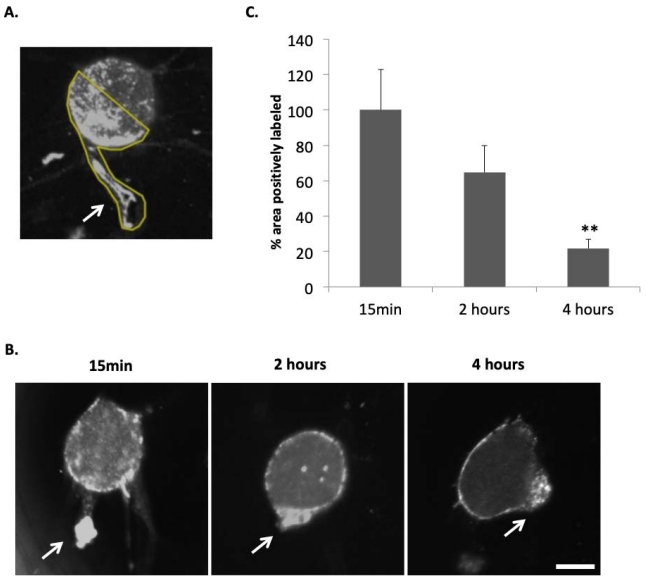

FIGURE 4. The barbed end assay demonstrates changes in free barbed ends of actin filaments in rod photoreceptor terminals after retinal detachment and dissociation. (**A**) Rod cells were imaged with confocal microscopy. The free barbed ends were bound with biotin-actin subunits and labeled with anti-biotin Alexa 488 antibody. The region of interest (ROI) for each rod cell used for quantification of fluorescence is *outlined in yellow* and includes the terminal, axon if present, and the basal most portion of the nuclear pole to which the axon terminal retracts. *Arrow* points to the presynaptic terminal. (**B**) Examples of the barbed end signal in rod photoreceptors after 15 minutes, 2 and 4 hours in culture (approximately 1, 3, and 5 hours after detachment). *Arrows*, presynaptic terminals. (**C**) Quantification of fluorescent signal for F-actin barbed ends. Percentage area of total ROI with positive labeling for F-actin barbed ends was measured and normalized (control group set at 100%). Signal in basal (axonal) region of rod cells appeared highest at 15 minutes of culture (set arbitrarily at 100%) and decreased significantly by 4 hours. Optical sections, 1 μm. *Scale bar*: 10 μm. $n = 3$ animals, 9 culture dishes, 60 rod cells; 1-way ANOVA, $^{**}P < 0.01$.

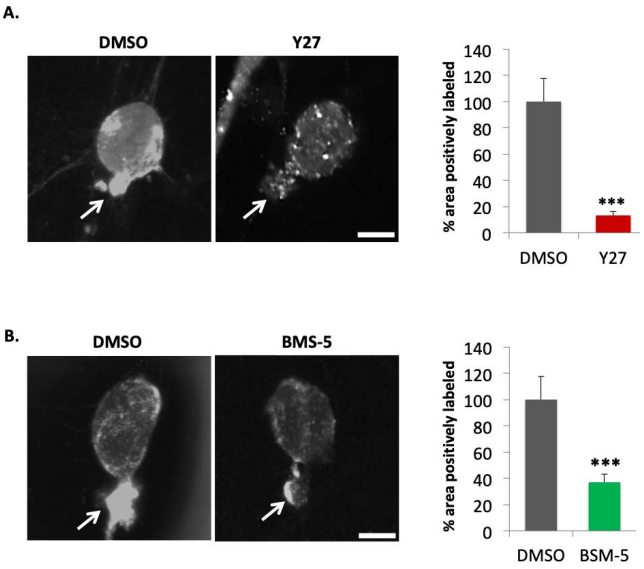

FIGURE 5. ROCK-LIMK inhibition significantly decreases the production of actin barbed ends in the axonal region of rod photoreceptors. Retinas were pretreated with inhibitors (**A**, 30 μM Y27632; **B**, 10 μM BMS-5) for 20 minutes before retinal detachment, then dissociated, plated, and examined by the barbed end assay after a 15 minutes incubation. DMSO, control. (**A**) *Left*, representative cells for control and ROCK inhibition (Y27). *Arrows*, presynaptic terminals. *Right*, quantification of barbed end signal in ROI (the same as Fig. 4A). (**B**) *Left*, representative cells for control and LIMK inhibition (BMS-5). *Arrows*, presynaptic terminals. *Right*, quantification of barbed end signal in ROI (the same as Fig. 4A). Optical sections, 1 μm. *Scale bars*: 10μm. $n = 6$ animals, 12 culture dishes, 113 rod cells; Student's *t*-test, $^{***}P < 0.001$.

These results further support our hypothesis that actin reorganization is a component of the machinery that regulates axon retraction of rod photoreceptor after injury.

Discussion

Although the rearrangement of actin cytoskeleton is implied in the injury-induced axonal plasticity of rod photoreceptors due to the obvious structural changes, a clear demonstration of actin's contribution to axon retraction has been absent. Previous studies demonstrated the role of ROCK and LIMK activity in promoting axon retraction[5,6,33] and led to the idea that both actomyosin contraction (through ROCK activation of myosin light chain) and actin filament turnover (through LIMK phosphorylation of cofilin, which regulates actin filament stability) were important.

In this study, we explored the role of actin filament assembly/disassembly in synaptic retraction of injured photoreceptors. Our results confirmed that (1) LIMK-cofilin activity promotes actin filament depolymerization in rod photoreceptors, and (2) this increased filament depolymerization contributes to rod axon retraction after injury.

Although we have looked at axon retraction during the first 24 hours after detachment, we focused on the first few hours for several reasons: (1) Activation of RhoA in retinal explants significantly increases only 10 minutes after detachment in vitro. In addition, while activation continues for 24 hours, peak activity occurs rapidly, 2 hours after detachment (Wang J, et al. *IOVS* 2013;54:ARVO E-Abstract 2845).[11] (2) Although retraction by most isolated rod cells occurs during the first 24 hours in vitro with axons being subsumed into the cell body, the highest rate of retraction (about 2 μm/hr) occurs during the first 6 hours of culture after isolation.[5] (3) After detachment in vivo, we have recently reported that significant RhoA activation and rod cell axon retraction are present early, by 2 hours after the injury.[11] The present report adds to the list of early events; phosphorylation of cofilin significantly increased 30 minutes after detachment, and the barbed end assay showed more fluorescence after 15 minutes in culture (about 1 hour after detachment) than after 4 hours.

If we combine our past and present results, they suggest the following scenario regarding actin filament dynamics: After detachment, RhoA is activated to phosphorylate ROCK, which in turn activates/phosphorylates LIMK. LIMK then phosphorylates cofilin. Because there are no changes in total cofilin, the ratio of p-cofilin to non-phosphorylated cofilin increases, resulting in a reduction of cofilin binding to actin filaments, breakage of actin filaments, and an increase in barbed ends.

Understanding of the activities of cofilin in other systems supports the above scenario. Cofilin binds to mature actin filaments with high affinity in its non-phosphorylated form; upon phosphorylation by LIMK, cofilin can be released from actin filaments. At the boundary of the bare and the cofilin-decorated actin filament, mechanical discontinuity occurs. Such discontinuity is vulnerable to stress and accounts for cofilin-dependent actin filament severing.[34,40–43] The key to actin regulation by cofilin lies in the relative concentration between non-phosphorylated (active) cofilin and actin filaments: At high concentrations of unphosphorylated cofilin,

Investigative Ophthalmology & Visual Science

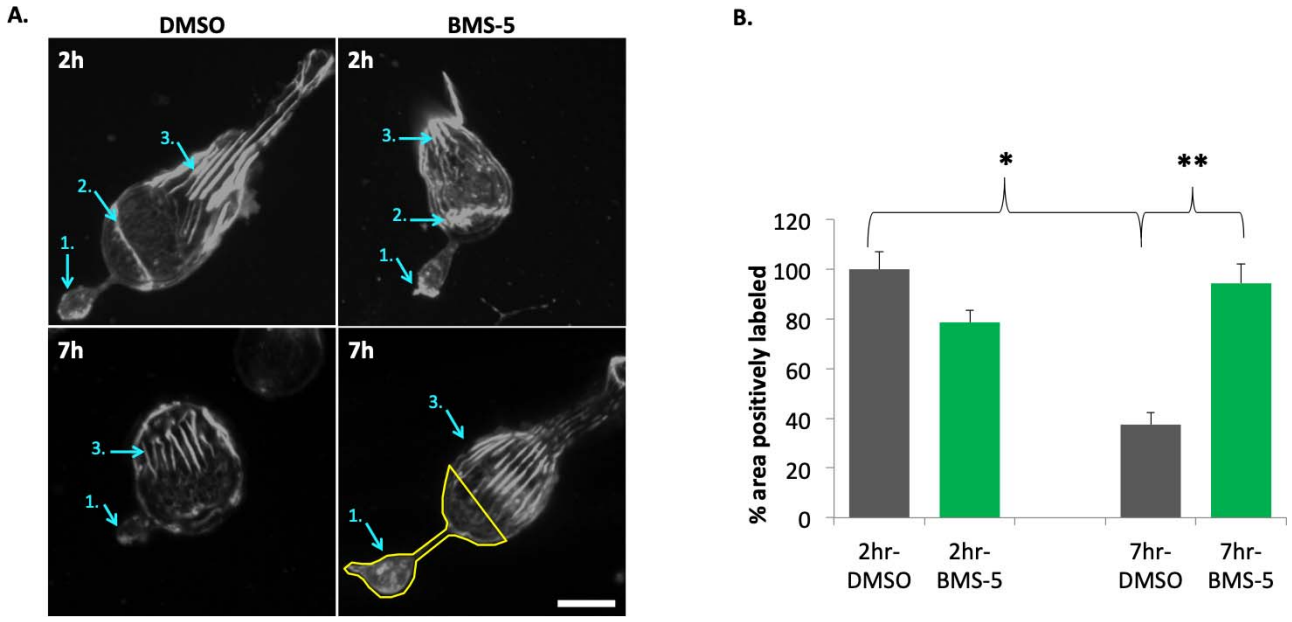

Figure 6. LIMK inhibition (10 μM BMS-5) stabilizes actin filaments in the basal (axonal) region of rod photoreceptors after injury. (**A**) Examples of actin filament staining with phalloidin in rod photoreceptors, 2 and 7 hours in control (DMSO) and treated (BMS-5) cultures. Cell in 2 hour-control has an outer segment. *Arrows*: 1, axon terminal; 2, zonula adherens; 3, calycal processes. *Lower right panel* indicates the ROI (outlined in *yellow*) used for quantification, which includes the terminal, axon if present, and the basal-most portion of the nuclear pole to which the axon terminal retracts. Comparison of treated and control cells at 2 hours and 7 hours shows that the actin filaments in the calycal processes remained structurally intact in the presence or absence of an outer segment. (**B**) Quantification of fluorescent signal for F-actin in ROI of rod cells at 2 and 7 hours in culture. Percentage of total ROI area with positive labeling for F-actin was measured and normalized (control group set at 100%). In control, a significant loss of staining at 7 hours suggests depolymerization of actin filaments has occurred. BMS-5 prevents this loss. Optical sections, 1 μm. *Scale bar*: 10 μm. $n = 3$ animals, 12 culture dishes, 101 rod cells; 1-way ANOVA with post hoc Tukey's test, $^{*}P < 0.05$, $^{**}P < 0.01$.

filament stabilization or nucleation occurs; at low concentrations, actin filament disassembly occurs.[44] In the retina, increased p-cofilin in Western blots suggests that actin filament disassembly occurs after detachment, whereas confocal microscopy confirmed the presence of p-cofilin specifically in rod photoreceptors terminals. This observation is consistent with published evidence that RhoA and LIMK are also present in rod terminals.[5,33]

Finally, although either ROCK or LIMK inhibition significantly reduced phosphorylation of cofilin after injury, indicating that the activity of these kinases increases p-cofilin, this does not rule out the possibility that the increased p-cofilin is also partially due to a reduction of SSH activity. Studies have reported that the phosphatase SSH is under several regulatory mechanisms,[45–47] but its regulation in photoreceptors remains to be investigated. Presently, the individual contributions of LIMK and SSH to phosphorylation of cofilin in the context of injury-induced photoreceptor synaptic plasticity are unclear.

Activity of LIMK in other systems also supports our scenario. LIMK activity has been reported to promote cell motility and morphological change in various cell types, including neurons.[30,37,48–56] In axon growth cones, for instance, phosphorylation of cofilin by LIMK is necessary for Sema 3A-induced collapse.[37] Moreover, mathematical simulations indicate that LIMK-dependent cofilin phosphorylation amplifies actin-severing activity locally.[42]

Actin filament turnover in the synaptic terminal of rod photoreceptors after injury was more directly examined in single cells through barbed end assays. Mature actin filaments usually bind capping proteins at their barbed ends. Severing by cofilin causes generation of free barbed ends, which allow subsequent assembly and possibly some disassembly.[57] In the axon terminals of isolated rod photoreceptors, a high level of barbed end labeling was detected initially, which subsided gradually. The decline in the barbed end signal was possibly due to either increased binding of capping proteins to the free barbed ends or due to reduced levels of ROCK and LIMK activity since we observed that inhibition of these kinases decreases the production of barbed ends. Future studies may be able to determine the localization and quantification of capping proteins during axon retraction after injury.

Following this analysis, increases in barbed ends should affect the pool of filamentous actin and, indeed, a reduction in labeling for actin filaments with phalloidin was observed during the initial period of rapid axon retraction by isolated rod cells. LIMK inhibition and Cyto D prevented this reduction. LIMK inhibition in isolated cells presumably reduced cofilin phosphorylation (as it had in retinal explants), leaving actin filaments protected by non-phosphorylated cofilin. Cyto D, however, is known to block polymerization and depolymerization in vitro by binding to the barbed ends with high affinity and actin monomers with low affinity when in high concentration.[38,39] Although the conventional view is that Cyto D prevents turnover of actin filaments and thus stabilizes actin cytoskeleton; in intact cells, Cyto D can have a variety of effects, including polymerization, depolymerization, or disorganization of actin filaments.[36,58–63] In isolated rod cells, the decrease of axon retraction and the increase in phalloidin labeling induced by cytochalasin D is likely due to a disruption in actin depolymerization.

In summary, the mechanisms that cause disjunction of the rod presynaptic terminal from its postsynaptic partners appear to include F-actin depolymerization, as well as actomyosin contraction[2,58]; however, other activities (such as loss of cell-to-cell adhesion) must also be involved. In retinal ganglion cell axons, depolymerization occurs in response to RhoA-promoted axon retraction induced by ephrin-A2; additionally, there is a concomitant decrease in F-actin turnover and thereby a

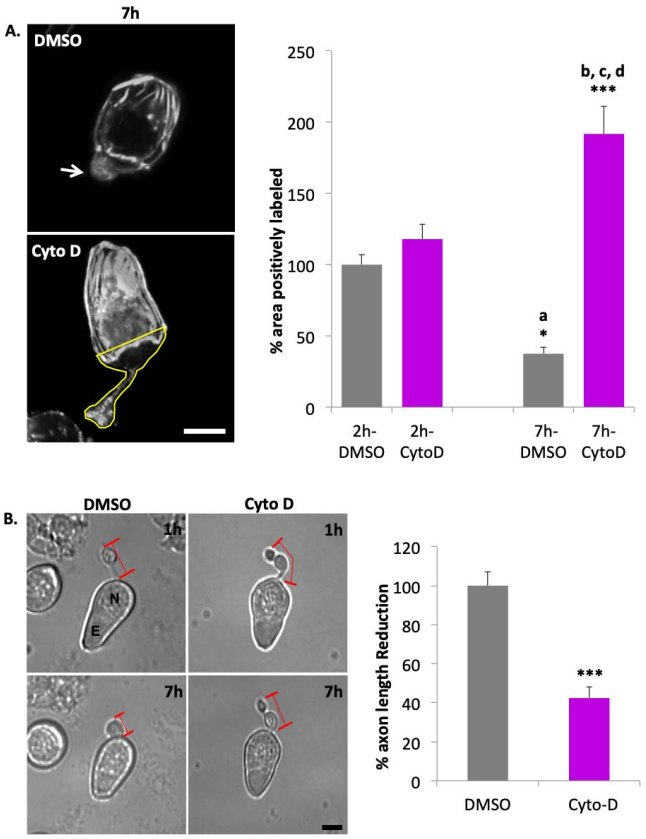

Figure 7. Cytochalasin D (1 μM Cyto D) reduces loss of actin filaments in the basal region of rod photoreceptors and axon retraction after injury. (**A**) *Left*, representative actin filament labeling with phalloidin in rod photoreceptors after 7 hours in culture (Control, *upper image*; Cyto D treatment, *lower image*; *arrow*, axon terminal). *Lower image* indicates the ROI (outlined in *yellow*) for quantification, which includes the terminal, axon if present, and the basal-most portion of the nuclear pole to which the axon terminal retracts. *Right*, quantification of percent area of labeled actin filaments of the total area in basal regions of rod cells (the same as Fig. 6B) of 2- and 7-hour cultures, with and without Cyto D. Optical sections, 1 μm. *Scale bar*: 10 μm. $n = 3$ animals, 12 culture dishes, 117 rod cells; 1-way ANOVA with post hoc Tukey's test, $^{*}P < 0.05$, $^{***}P < 0.001$; post hoc Tukey's test, a: 2h-DMSO vs. 7h-DMSO, <0.05; b, c, d: 7h-Cyto D vs. 2h-DMSO, 2h-Cyto D, and 7h-DMSO, <0.001. (**B**) *Left*, representative rod photoreceptors in culture 1 and 7 hours, with DMSO or Cyto D treatment. *Red lines* indicate length of axon. N, nucleus; E, ellipsoid. *Scale bar*: 10 μm. *Right*, Cyto D reduced axon retraction by ~40% over 7 hours. % Length reduction = (L1 – L7) ÷ L1 × 100%; L1, axon length at 1-hour culture; L7, axon length at 7 hours culture. All data were normalized to control group, which was set as 100%. $n = 3$ animals, 6 culture dishes, 150 rod cells; Student's *t*-test, $^{***}P < 0.001$.

stabilization of remaining actin filaments.[59] In other words, there is severing of filaments without polymerization for a portion of the F-actin. Remaining filaments participate in actomyosin contractility. Thus, rod cells appear to use mechanisms also seen in axonal growth cone collapse and retraction,[60] even though some of their presynaptic molecular components are unique to ribbon synapses.

Cone cells are not known to show axon retraction in response to injury (retinal detachment); however, they do exhibit shape changes and loss of connectivity with bipolar cells at their ribbon synapses, which can be devastating to vision.[61,62] Cone cell axonal processes, like rod cells, are sensitive to RhoA activity[5] but have microtubule associated proteins and calcium channels that differ from rod cells.[15,63–66] These molecular differences may modify the form of cone structural responses. Hair cells of the auditory system, which contact spiral ganglion cells at ribbon synapses, also have injury responses that result in synaptic disjunction. The relevant insult is loud noise. For the auditory system, ribbon active zones are abandoned as ganglionic dendrites retract.[67] Additionally, bipolar-ganglion cell ribbon synapses in the retina are affected by glaucoma and show a reduction in active zone size with disease.[68] Thus, ribbon synapses of a variety of critical sensory (and sensory-related) neurons exhibit injury-induced synaptopathy. For rod photoreceptors, we are beginning to understand the mechanisms leading to synaptic disjunction and develop therapeutic strategies by blocking RhoA signaling to preserve their synapses.[25]

Acknowledgments

The authors thank Frank Kung and Jianfeng Wang for assistance with double-blind analysis and Ilene Sugino for assistance with confocal microscopy.

Supported by National Institutes of Health Grant EY021542 and the F.M. Kirby Foundation. The authors alone are responsible for the content and writing of the paper.

Disclosure: **W. Wang**, None; **E. Halasz**, None; **E. Townes-Anderson**, None

References

1. Linberg KA, Lewis GP, Fisher SK. Retraction and remodeling of rod spherules are early events following experimental retinal detachment: an ultrastructural study using serial sections. *Mol Vis*. 2009;15:10–25.
2. Wang J, Zarbin M, Sugino I, Whitehead I, Townes-Anderson E. RhoA signaling and synaptic damage occur within hours in a live pig model of CNS injury, retinal detachment. *Invest Ophthalmol Vis Sci*. 2016;57:3892–3906.
3. Erickson PA, Fisher SK, Anderson DH, Stern WH, Borgula GA. Retinal detachment in the cat: the outer nuclear and outer plexiform layers. *Invest Ophthalmol Vis Sci*. 1983;24:927–942.
4. Fisher SK, Lewis GP. Muller cell and neuronal remodeling in retinal detachment and reattachment and their potential consequences for visual recovery: a review and reconsideration of recent data. *Vision Res*. 2003;43:887–897.
5. Fontainhas AM, Townes-Anderson E. RhoA and its role in synaptic structural plasticity of isolated salamander photoreceptors. *Invest Ophthalmol Vis Sci*. 2008;49:4177–4187.
6. Fontainhas AM, Townes-Anderson E. RhoA inactivation prevents photoreceptor axon retraction in an in vitro model of acute retinal detachment. *Invest Ophthalmol Vis Sci*. 2011;52:579–587.
7. Lewis GP, Charteris DG, Sethi CS, Fisher SK. Animal models of retinal detachment and reattachment: identifying cellular events that may affect visual recovery. *Eye (Lond)*. 2002;16:375–387.
8. Guerin CJ, Lewis GP, Fisher SK, Anderson DH. Recovery of photoreceptor outer segment length and analysis of membrane assembly rates in regenerating primate photoreceptor outer segments. *Invest Ophthalmol Vis Sci*. 1993;34:175–183.
9. Burton TC. Recovery of visual acuity after retinal detachment involving the macula. *Trans Am Ophthalmol Soc*. 1982;80:475–497.
10. Tani P, Robertson DM, Langworthy A. Rhegmatogenous retinal detachment without macular involvement treated with scleral buckling. *Am J Ophthalmol*. 1980;90:503–508.

11. Wang W, Townes-Anderson E. Lim kinase, a bi-functional effector in injury-induced structural plasticity of synapses. *Neural Regen Res*. 2016;11:1029–1032.
12. Marc RE, Jones BW, Watt CB, Strettoi E. Neural remodeling in retinal degeneration. *Prog Retin Eye Res*. 2003;22:607–655.
13. Wang W, Townes-Anderson E. LIM kinase, a newly identified regulator of presynaptic remodeling by rod photoreceptors after injury. *Invest Ophthalmol Vis Sci*. 2015;56:7847–7858.
14. Maekawa M, Ishizaki T, Boku S, et al. Signaling from Rho to the actin cytoskeleton through protein kinases ROCK and LIM-kinase. *Science*. 1999;285:895–898.
15. Tucker RP, Matus AI. Microtubule-associated proteins characteristic of embryonic brain are found in the adult mammalian retina. *Dev Biol*. 1988;130:423–434.
16. Nachman-Clewner M, St Jules R, Townes-Anderson E. L-type calcium channels in the photoreceptor ribbon synapse: localization and role in plasticity. *J Comp Neurol*. 1999;415:1–16.
17. Mandell JW, MacLeish PR, Townes-Anderson E. Process outgrowth and synaptic varicosity formation by adult photoreceptors in vitro. *J Neurosci*. 1993;13:3533–3548.
18. Schlamp CL, Williams DS. Myosin V in the retina: localization in the rod photoreceptor synapse. *Exp Eye Res*. 1996;63:613–619.
19. Khodair MA, Zarbin MA, Townes-Anderson E. Synaptic plasticity in mammalian photoreceptors prepared as sheets for retinal transplantation. *Invest Ophthalmol Vis Sci*. 2003;44:4976–4988.
20. MacLeish PR, Townes-Anderson E. Growth and synapse formation among major classes of adult salamander retinal neurons in vitro. *Neuron*. 1988;1:751–760.
21. Nachman-Clewner M, Townes-Anderson E. Injury-induced remodelling and regeneration of the ribbon presynaptic terminal in vitro. *J Neurocytol*. 1996;25:597–613.
22. MacLeish PR, Barnstable CJ, Townes-Anderson E. Use of a monoclonal antibody as a substrate for mature neurons in vitro. *Proc Natl Acad Sci U S A*. 1983;80:7014–7018.
23. Prince JH, Ruskell GL. The use of domestic animals for experimental ophthalmology. *Am J Ophthalmol*. 1960;49:1202–1207.
24. Simoens P, De Schaepdrijver L, Lauwers H. Morphologic and clinical study of the retinal circulation in the miniature pig. A: morphology of the retinal microvasculature. *Exp Eye Res*. 1992;54:965–973.
25. Townes-Anderson E, Wang J, Halasz E, et al. Fasudil, a clinically used ROCK inhibitor, stabilizes rod photoreceptor synapses after retinal detachment. *Trans Vis Sci Tech*. 2017;6(3):22.
26. Yamaguchi H, Miwa Y, Kasa M, et al. Structural basis for induced-fit binding of Rho-kinase to the inhibitor Y-27632. *J Biochem*. 2006;140:305–311.
27. Jacobs M, Hayakawa K, Swenson L, et al. The structure of dimeric ROCK I reveals the mechanism for ligand selectivity. *J Biol Chem*. 2006;281:260–268.
28. Ross-Macdonald P, de Silva H, Guo Q, et al. Identification of a nonkinase target mediating cytotoxicity of novel kinase inhibitors. *Mol Cancer Ther*. 2008;7:3490–3498.
29. Scott RW, Hooper S, Crighton D, et al. LIM kinases are required for invasive path generation by tumor and tumor-associated stromal cells. *J Cell Biol*. 2010;191:169–185.
30. Park JB, Agnihotri S, Golbourn B, et al. Transcriptional profiling of GBM invasion genes identifies effective inhibitors of the LIM kinase-Cofilin pathway. *Oncotarget*. 2014;5:9382–9395.
31. Li M, Huang Y, Ma AA, Lin E, Diamond MI. Y-27632 improves rotarod performance and reduces huntingtin levels in R6/2 mice. *Neurobiol Dis*. 2009;36:413–420.
32. Townes-Anderson E, MacLeish PR, Raviola E. Rod cells dissociated from mature salamander retina: ultrastructure and uptake of horseradish peroxidase. *J Cell Biol*. 1985;100:175–188.
33. Wang B, Ding YM, Wang CT, Wang WX. Role of ROCK expression in gallbladder smooth muscle contraction. *Mol Med Rep*. 2015;12:2907–2911.
34. Elam WA, Kang H, De la Cruz EM. Biophysics of actin filament severing by cofilin. *FEBS Lett*. 2013;587:1215–1219.
35. Courtemanche N, Gifford SM, Simpson MA, Pollard TD, Koleske AJ. Abl2/Abl-related gene stabilizes actin filaments, stimulates actin branching by actin-related protein 2/3 complex, and promotes actin filament severing by cofilin. *J Biol Chem*. 2015;290:4038–4046.
36. Bravo-Cordero JJ, Magalhaes MAO, Eddy RJ, Hodgson L, Condeelis J. Functions of cofilin in cell locomotion and invasion. *Nat Rev Mol Cell Biol*. 2013;14:405–415.
37. Aizawa H, Wakatsuki S, Ishii A, et al. Phosphorylation of cofilin by LIM-kinase is necessary for semaphorin 3A-induced growth cone collapse. *Nat Neurosci*. 2001;4:367–373.
38. Paavilainen VO, Bertling E, Falck S, Lappalainen P. Regulation of cytoskeletal dynamics by actin-monomer-binding proteins. *Trends Cell Biol.* 2004;14:386–394.
39. Shoji K, Ohashi K, Sampei K, Oikawa M, Mizuno K. Cytochalasin D acts as an inhibitor of the actin-cofilin interaction. *Biochem Biophys Res Commun.* 2012;424:52–57.
40. Bobkov AA, Muhlrad A, Kokabi K, Vorobiev S, Almo SC, Reisler E. Structural effects of cofilin on longitudinal contacts in F-actin. *J Mol Biol*. 2002;323:739–750.
41. Bobkov AA, Muhlrad A, Shvetsov A, et al. Cofilin (ADF) affects lateral contacts in F-actin. *J Mol Biol*. 2004;337:93–104.
42. Bravo-Cordero JJ, Magalhaes MA, Eddy RJ, Hodgson L, Condeelis J. Functions of cofilin in cell locomotion and invasion. *Nat Rev Mol Cell Biol*. 2013;14:405–415.
43. Cao W, Goodarzi JP, De La Cruz EM. Energetics and kinetics of cooperative cofilin-actin filament interactions. *J Mol Biol*. 2006;361:257–267.
44. Andrianantoandro E, Pollard TD. Mechanism of actin filament turnover by severing and nucleation at different concentrations of ADF/cofilin. *Mol Cell*. 2006;24:13–23.
45. Eiseler T, Doppler H, Yan IK, Kitatani K, Mizuno K, Storz P. Protein kinase D1 regulates cofilin-mediated F-actin reorganization and cell motility through slingshot. *Nat Cell Biol*. 2009;11:545–556.
46. Soosairajah J, Maiti S, Wiggan O, et al. Interplay between components of a novel LIM kinase-slingshot phosphatase complex regulates cofilin. *EMBO J*. 2005;24:473–486.
47. Wang Y, Shibasaki F, Mizuno K. Calcium signal-induced cofilin dephosphorylation is mediated by Slingshot via calcineurin. *J Biol Chem*. 2005;280:12683–12689.
48. Ding Z, Joy M, Bhargava R, et al. Profilin-1 downregulation has contrasting effects on early vs late steps of breast cancer metastasis. *Oncogene*. 2014;33:2065–2074.
49. Edwards DC, Gill GN. Structural features of LIM kinase that control effects on the actin cytoskeleton. *J Biol Chem*. 1999;274:11352–11361.
50. Foletta VC, Moussi N, Sarmiere PD, Bamburg JR, Bernard O. LIM kinase 1, a key regulator of actin dynamics, is widely expressed in embryonic and adult tissues. *Exp Cell Res*. 2004;294:392–405.
51. Heredia L, Helguera P, de Olmos S, et al. Phosphorylation of actin-depolymerizing factor/cofilin by LIM-kinase mediates amyloid beta-induced degeneration: a potential mechanism of neuronal dystrophy in Alzheimer's disease. *J Neurosci*. 2006;26:6533–6542.

Investigative Ophthalmology & Visual Science

52. Hocking JC, Hehr CL, Bertolesi G, Funakoshi H, Nakamura T, McFarlane S. LIMK1 acts downstream of BMP signaling in developing retinal ganglion cell axons but not dendrites. *Dev Biol*. 2009;330:273–285.
53. Jiang H, Guo W, Liang X, Rao Y. Both the establishment and the maintenance of neuronal polarity require active mechanisms: critical roles of GSK-3beta and its upstream regulators. *Cell*. 2005;120:123–135.
54. Manetti F. LIM kinases are attractive targets with many macromolecular partners and only a few small molecule regulators. *Med Res Rev*. 2012;32:968–998.
55. Ohashi K, Hosoya T, Takahashi K, Hing H, Mizuno K. A Drosophila homolog of LIM-kinase phosphorylates cofilin and induces actin cytoskeletal reorganization. *Biochem Biophys Res Commun*. 2000;276:1178–1185.
56. Piccioli ZD, Littleton JT. Retrograde BMP signaling modulates rapid activity-dependent synaptic growth via presynaptic LIM kinase regulation of cofilin. *J Neurosci*. 2014;34:4371–4381.
57. Wioland H, Guichard B, Senju Y, et al. ADF/cofilin accelerates actin dynamics by severing filaments and promoting their depolymerization at both ends. *Curr Biol*. 2017;27:1956–1967.
58. Wang W, Townes-Anderson E. Lim kinase, a bi-functional effector in injury-induced structural plasticity of synapses. *Neural Regen Res*. 2016;11:1029–1032.
59. Gallo G, Yee HF Jr, Letourneau PC. Actin turnover is required to prevent axon retraction driven by endogenous actomyosin contractility. *J Cell Biol*. 2002;158:1219–1228.
60. Gallo G, Letourneau PC. Regulation of growth cone actin filaments by guidance cues. *J Neurobiol*. 2004;58:92–102.
61. Fisher SK, Stone J, Rex TS, Linberg KA, Lewis GP. Experimental retinal detachment: a paradigm for understanding the effects of induced photoreceptor degeneration. *Prog Brain Res*. 2001;131:679–698.
62. Fisher SK, Lewis GP, Linberg KA, Verardo MR. Cellular remodeling in mammalian retina: results from studies of experimental retinal detachment. *Prog Retin Eye Res*. 2005;24:395–431.
63. Tucker RP, Binder LI, Matus AI. Differential localization of the high- and low-molecular weight variants of MAP2 in the developing retina. *Brain Res*. 1988;466:313–318.
64. Taylor WR, Morgans C. Localization and properties of voltage-gated calcium channels in cone photoreceptors of *Tupaia belangeri*. *Vis Neurosci*. 1998;15:541–552.
65. Morgans CW. Localization of the alpha(1F) calcium channel subunit in the rat retina. *Invest Ophthalmol Vis Sci*. 2001;42:2414–2418.
66. Krizaj D, Lai FA, Copenhagen DR. Ryanodine stores and calcium regulation in the inner segments of salamander rods and cones. *J Physiol*. 2003;547:761–774.
67. Kujawa SG, Liberman MC. Adding insult to injury: cochlear nerve degeneration after "temporary" noise-induced hearing loss. *J Neurosci*. 2009;29:14077–14085.
68. Park HY, Kim JH, Park CK. Alterations of the synapse of the inner retinal layers after chronic intraocular pressure elevation in glaucoma animal model. *Mol Brain*. 2014;7:53.

Investigative Ophthalmology & Visual Science